1. AGENCY USE ONLY (Leave blank)	TE	3. REPORT TYPE AND DATES COVERED
	March-April 1993	Journal article reprint

4. TITLE AND SUBTITLE

Schlieren Studies of Compressibility Effects on Dynamic Stall of Transiently Pitching Airfoils

5. FUNDING NUMBERS

ARO MIPR 125-93

6. AUTHOR(S)

M.S. Chandrasekhara, S. Ahmed, L.W. Carr

7. PERFORMING ORGANIZATION NAME(S) AND ADDRESS(ES)

Navy-NASA Joint Institute of Aeronautics. Code AA/CH
Dept. of Aeronautics and Astronautics
Naval Postgraduate School, Monterey, CA 93943

8. PERFORMING ORGANIZATION REPORT NUMBER

9. SPONSORING/MONITORING AGENCY NAME(S) AND ADDRESS(ES)

U. S. Army Research Office
P.O. Box 12211
Research Triangle Park, NC 27709-2211

10. SPONSORING/MONITORING AGENCY REPORT NUMBER

ARO 27894.17-EG

11. SUPPLEMENTARY NOTES

The view, opinions and/or findings contained in this report are those of the author(s) and should not be construed as an official Department of the Army position, policy, or decision, unless so designated by other documentation.

12a. DISTRIBUTION/AVAILABILITY STATEMENT

Approved for public release; distribution unlimited.

12b. DISTRIBUTION CODE

13. ABSTRACT (Maximum 200 words)

Compressibility effects on the flowfield of an airfoil executing rapid transient pitching motion from 0-60 deg over a wide range of Mach numbers and pitching rates were studied using a stroboscopic schlieren flow visualization technique. The studies have led to the first direct experimental documentation of multiple shocks on the airfoil upper surface flow for certain conditions. Also, at low Mach numbers, additionai coherent vortical structures were found to be present along with the dynamic stall vortex, whereas at higher Mach numbers the flow was dominated by a single vortex. The delineating Mach number for significant compressibility effects was 0.3 and the dynamic stall process was accelerated by increasing the Mach number above that value. Increasing the pitch rate monotonically delayed stall to angles of attack as large as 27 deg.

14. SUBJECT TERMS	15. NUMBER OF PAGES
Dynamic stall. Transiently pitching airfoils. Stroboscopic Schlieren	9
	16. PROCE CODE

17. SECURITY CLASSIFICATION OF REPORT	18. SECURITY CLASSIFICATION OF THIS PAGE	19. SECURITY CLASSIFICATION OF ABSTRACT	20. LIMITATION OF ABSTRACT
UNCLASSIFIED	UNCLASSIFIED	UNCLASSIFIED	UL

NSN
7540-01-280-5500

Standard Form 298 (Rev. 2-89)
Prescribed by ANSI Std. 239-18
298-102

Schlieren Studies of Compressibility Effects on Dynamic Stall of Transiently Pitching Airfoils

M. S. Chandrasekhara, S. Ahmed, L. W. Carr

Reprinted from

Journal of Aircraft

Volume 30, Number 2, March–April 1993, Pages 213–220

AIAA

A publication of the
American Institute of Aeronautics and Astronautics, Inc.
The Aerospace Center, 370 L'Enfant Promenade, SW
Washington, DC 20024-2518

JOURNAL OF AIRCRAFT
Vol. 30, No. 2, March–April 1993

Schlieren Studies of Compressibility Effects on Dynamic Stall of Transiently Pitching Airfoils

M. S. Chandrasekhara*
Naval Postgraduate School, Monterey, California 93943
S. Ahmed†
MCAT Institute, San Jose, California 95127
and
L. W. Carr‡
NASA Ames Research Center, Moffett Field, California 94035

Compressibility effects on the flowfield of an airfoil executing rapid transient pitching motion from 0–60 deg over a wide range of Mach numbers and pitching rates were studied using a stroboscopic schlieren flow visualization technique. The studies have led to the first direct experimental documentation of multiple shocks on the airfoil upper surface flow for certain conditions. Also, at low Mach numbers, additional coherent vortical structures were found to be present along with the dynamic stall vortex, whereas at higher Mach numbers the flow was dominated by a single vortex. The delineating Mach number for significant compressibility effects was 0.3 and the dynamic stall process was accelerated by increasing the Mach number above that value. Increasing the pitch rate monotonically delayed stall to angles of attack as large as 27 deg.

Nomenclature

c	=	airfoil chord
M	=	freestream Mach number
U_∞	=	freestream velocity
x	=	chordwise distance
α	=	angle of attack
$\dot{\alpha}$	=	pitch rate, deg/s
α^+	=	$\dot{\alpha}c/U_\infty$, nondimensional pitch rate

I. Introduction

THERE is considerable interest in the enhancement and sustenance of lift by dynamically pitching an airfoil in applications related to fixed wing aircraft supermaneuverability and enhanced agility. The production of dynamic lift by rapid unsteady motion such as oscillatory pitching or ramp-type pitching is well known. Carr[1] provides a comprehensive review of the problem and related processes. Over the years significant effort has been devoted to obtaining details of the process of dynamic lift generation over a rapidly pitching airfoil, e.g., to quantify it and identify the parameters affecting it.[2] A survey of the available literature reveals that the process of dynamic stall is strongly dependent on the airfoil geometry (in particular the leading-edge shape), Mach number, degree of unsteadiness or nondimensional pitch rate, Reynolds number, state of the airfoil boundary layer, airfoil initial angle of attack before pitching, three-dimensionality, type of airfoil motion, location of pitch point, etc. The various aspects of the problem have been studied by several researchers. Freymuth[3] provides excellent flow visualization pictures at low speeds. Lorber and Carta,[4] Albertson et al.,[5] Walker et al.,[6] among others have measured the surface pressure distributions. Francis and Keese[7] have found that the maximum lift coefficient increases monotonically until a nondimensional pitch rate of 0.025, it decreases thereafter. Jumper et al.[8] concluded from their studies that the pivot point has a large effect on dynamic stall. Harper and Flanigan[9] found that as the Mach number is increased, the dynamic lift overshoot steadily decreases and finally ceases at $M \approx 0.6$. Whereas, these above-mentioned studies are experimental, there are some computational studies (Ekaterinaris,[10] Visbal,[11] among others) that have produced good agreement with the available data.

The phenomenon of dynamic stall is characterized primarily by a clockwise vortex (for flow moving from left to right) that is produced by the large amount of coherent vorticity created near the leading-edge region of rapidly pitching airfoils by the unsteady motion. In fact for certain flow conditions, Walker et al.[6] observed that two vortices are present on the airfoil. During the early stages of the stall process the flow around the airfoil remains attached, with the vortex being surrounded by the outer stream. As the angle of attack is increased well past the static stall angle, the vortex begins to grow and then convect over the upper surface. Eventually, when the vortex is shed into the wake, deep dynamic stall is said to occur. This sequence of events has been derived from flow visualization experiments at low Mach numbers. Computations and surface pressure measurements have shown that extremely large suction pressures develop in the region very close to the leading edge, pointing to the formation of locally supersonic regions. In fact, even at the low freestream Mach number of 0.2, the local flow can attain sonic values.[12] It is then likely that a shock can form in the flow. If it does it could have a dramatic effect on the dynamic stall process. However, until now there has been no direct experimental evidence of a shock, although its presence has been inferred from other measurements such as signatures of surface-mounted hot film gauges.[4] It is very clear that there is a strong need to obtain detailed experimental data about the influence of compressibility effects on

Received June 21, 1990; presented as Paper 90-3038 at the AIAA 8th Applied Aerodynamics Conference, Portland, OR, Aug. 20–22, 1990; revision received Feb. 18, 1992; accepted for publication March 8, 1992.

*Associate Director and Adjunct Professor, Navy-NASA Joint Institute of Aeronautics, Department of Aeronautics and Astronautics. Associate Fellow AIAA.

†Research Scientist, Navy-NASA Joint Institute of Aeronautics. Member AIAA.

‡Research Scientist and Group Leader, Unsteady Viscous Flows, Aeroflightdynamics Directorate, U.S. Army ATCOM and Fluid Mechanics Laboratory Branch. Member AIAA.

dynamic stall before a full understanding of the dynamic stall process can be obtained. This article presents some of the results of a visualization of the flow carried out using a stroboscopic schlieren method.

II. Description of the Experiment

A. Facility

The experiments were conducted in an in-draft wind tunnel of the Fluid Mechanics Laboratory (FML) at NASA Ames Research Center (ARC). It is one of the ongoing dynamic stall research projects of the Navy-NASA Joint Institute of Aeronautics between the Naval Postgraduate School and NASA ARC.

The details of the FML in-draft wind tunnel are given by Carr and Chandrasekhara.[13] The facility is one of a complex of four in-draft wind tunnels connected to an evacuation compressor. The test section size is 25 × 35 × 100 cm. The flow in the tunnel is controlled by a variable cross-section downstream diffuser. This throat is always kept choked so that no disturbances can propagate from the other tunnels or the compressor into the test section. The tunnel flow uniformity is ±0.25% at 58 m/s, with a turbulence intensity of 0.083% with a bandwidth of 5–50,000 Hz.[13]

An NACA 0012 airfoil with a chord of 7.62 cm is supported in a unique way by pins that are push fitted between two 2.54-cm-thick optical quality glass windows. The pins are smaller than the local airfoil thickness and, therefore, permit complete optical access to the airfoil surface. This makes detailed flow studies possible, even at the surface. The airfoil motion is produced by a hydraulic drive located on top of the test section which is connected to the window frames supporting the airfoil. Controlled movement of the hydraulic actuator provides the desired motion of the airfoil.

B. Details of the Hydraulic Actuator System

The following were specified as the requirements on the airfoil motion:

angle of attack α	0–60 deg
pitch rate $\dot{\alpha}$	0–3600 deg/s
acceleration rate	600,000 deg/s^2
change in α during acceleration	≤6 deg of pitch
time to reach constant $\dot{\alpha}$	≤4 ms
freestream Mach number	0.1–0.5
airfoil chord	7.62 cm
Reynolds number	2×10^5–10^6

It should be noted that at any Mach number, a 7.62-cm chord airfoil pitching at 3600 deg/s corresponds to a 3-m chord wing pitching at 90 deg/s, which is beyond the range of present day aircraft. Thus, results obtained from this study will make expansion of the flight envelope of both current and future aircraft systems possible. The maximum change in angle of attack to reach a constant pitch rate from rest at zero degrees angle of attack was specified to be less than 6 deg, so that the airfoil has reached a constant pitch rate well before the static stall angle was reached. To obtain reasonable experiment times, the system was also required to recycle 30 times a minute.

These exacting requirements meant that a powerful prime mover was necessary for this purpose. After considering several alternatives, a hydraulic drive system was found to be able to deliver the required performance. Such a system was designed taking into account the fact that the system characteristics are collectively determined by the interaction of the aerodynamic flowfield, the mechanical system with its linkages and associated backlash, and the hydraulic system with its leakage and the nonlinearities in each of these systems. The details of the feedback system design can be found in Ref. 14. Chandrasekhara and Carr[15] provide the other details of the final design, including those of the hydraulic circuit.

C. Instrumentation and Technique

The drive is equipped with its own instrumentation which is used by the feedback control system. These include a digital incremental position encoder (with a resolution of 0.03 deg/count) to provide the instantaneous angle of attack, and a linear (analog) velocity transducer for maintaining the airfoil velocity constant. The airfoil motion is software controlled from an IBM PC, with a motion controller card installed in one of its slots.

As stated earlier, the airfoil pitches from 0–60 deg at pitch rates up to 3600 deg/s and the motion is completed in 20 ms. Records of individual pitch-up motion were obtained using a MicroVAX II Work Station. The PC was linked to the MicroVAX with additional hardware to trigger data acquisition on the MicroVAX computer, with the third bit of the encoder providing the instantaneous angle-of-attack information. The third bit was chosen to prevent accidental triggering due to noise or similar uncontrollable parameters. Simultaneously, the internal clock of the computer was started so that the time history of the motion could be documented. Figure 1 shows typical plots of the variation of angle of attack with time for $M = 0.45$, a pitch rate $\dot{\alpha}$, of 3507 deg/s, and nondimensional pitch rate of $\alpha^+ = 0.03$; $M = 0.35$, $\dot{\alpha} = 2256$ deg/s, $\alpha^+ = 0.025$; and $M = 0.25$, $\dot{\alpha} = 1263$ deg/s, $\alpha^+ = 0.02$. Similar plots were obtained for all cases.

The schlieren instrumentation used is described by Carr and Chandrasekhara.[13] Flow visualization was obtained using the stroboscopic schlieren flow visualization technique. This involved triggering the schlieren light source at the desired instantaneous angle of attack by a specially designed electronic circuit. The encoder counts for the desired angle of attack was chosen as a BCD number by setting switches on the front panel of the hardware. The circuit included a comparator which output a TTL pulse when a match occurred between the selected count and the constantly changing encoder count. This pulse triggered the strobe light source and also latched the display of the encoder counts, thus permitting a check on and recording of the actual angle of attack at which

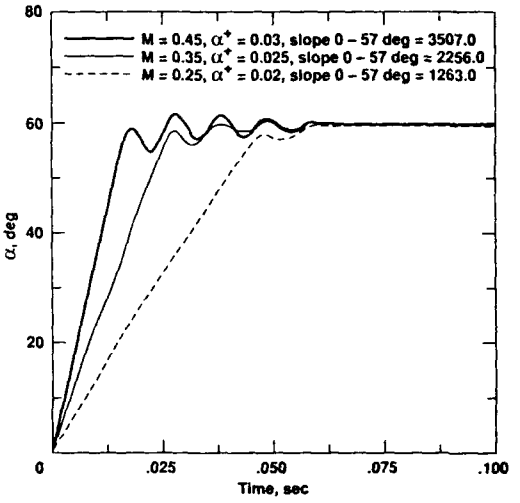

Fig. 1 Time history of pitching airfoil.

Table 1 Experimental conditions

	α^+						
M	0.01	0.02	0.025	0.03	0.035	0.04	0.05
0.20			X	X	X	X	X
0.25		X	X	X	X	X	X
0.30		X	X	X	X	X	
0.35		X	X	X	X	X	
0.40		X	X	X	X		
0.45	X	X	X	X			

the light flashed. No phase delays were found to be present in this process. The uncertainty in the flash timing was also verified to be nil by a light detecting photo diode which latched and froze the encoder display following the flashing of the strobe light. The flash duration was 1.5 μs.

The experiment consisted of running the tunnel at Mach numbers ranging from 0.2–0.45, while pitching the airfoil at rates from 1200–3600 deg/s, and taking the schlieren photographs. The resulting Reynolds number range was 400,000–900,000. The airfoil was oscillated about the $\frac{1}{4}c$ point. The matrix of experimental conditions is given in Table 1. Repeatability of the flow events was verified by obtaining several photographs of the flow for selected conditions, with virtually identical results for the conditions tested.

III. Results and Discussion

A. Stroboscopic Schlieren Flow Visualization Studies

Figures 2 and 3 present two sequences of stroboscopic schlieren photographs obtained for the cases of $M = 0.25$, $\alpha' = 0.05$, and $M = 0.45$, $\alpha' = 0.03$. These photographs were obtained by pitching the airfoil once for each frame shown. They represent the density gradients at the instant the photographs were taken without any history effects—unlike most other flow visualization photographs. The knife edge of the schlieren system was kept vertical for all cases.

The dominant feature in these figures is the presence of the dynamic stall vortex that appears as a dark circular region over the airfoil and moves along the airfoil upper surface and eventually past the trailing edge.

The dark region near the leading edge of the airfoil on its lower surface indicates the density gradients in the stagnating flow. As the angle of attack increases (up to 30 deg), the stagnation point moves downstream along the lower surface and stabilizes at ≈5% chord point. Also, as the angle of attack is increased, the dynamic stall vortex becomes distinct at $\alpha = 17$ deg in Fig. 2 at $M = 0.25$ and $\alpha' = 0.05$, and $\alpha = 13$ deg for the case of the higher Mach number of 0.45 and $\alpha' = 0.03$ in Fig. 3. In both cases, the vortex quickly grows into a large coherent structure. The boundary layer downstream of the vortex thickens with increasing angle of attack; at the same time, the leading-edge shear layer appears as a thin

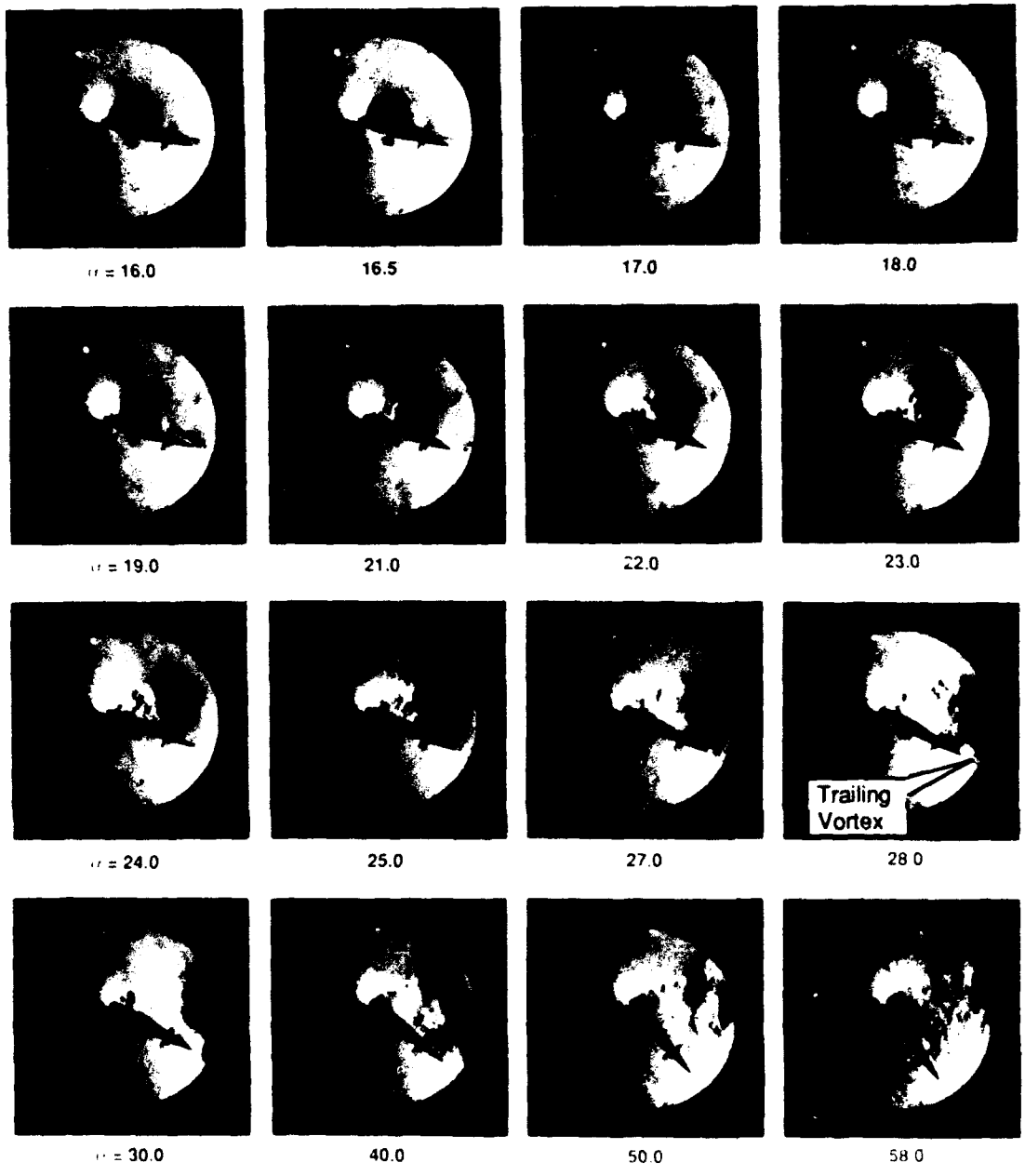

Fig. 2 Stroboscopic schlieren photographs of the compressibility effects on dynamic stall of a rapidly pitching airfoil: $M = 0.25$, $\alpha' = 0.05$.

streak (starting out initially as a dark layer and transforming into a lighter shade) and delineates the outer potential flow from the inner separated viscous layer. Ultimately the vortex is bounded by the edge of the shear layer upstream and by the boundary layer downstream. The flow downstream of the dynamic stall vortex is still attached as can be seen, e.g., in Fig. 3, $\alpha = 14.5$ deg. No trailing edge vortex was present on the airfoil for any of the cases studied. Walker et al.[6] have pointed out that the trailing edge vortex is due to the separating shear layer on the upper surface and is absent at higher Reynolds numbers, which is perhaps the reason why it was not found in the cases studied.

The vortex itself appears as a dark region as in its formative stages; the flow gradients in it have not fully developed. But when it grows and has acquired its terminal velocity it appears as a partially bright and partially dark image, with a sharp transition line where the local density gradient changes sign from negative to positive (light to dark) as can be seen in Fig. 2 for $\alpha = 21.0$ deg. For the case shown in Fig. 2, the flow stalls dynamically at $\alpha = 27$ deg (when the vortex has traveled past the trailing edge) and for $M = 0.45$ (Fig. 3) at $\alpha = 18$ deg. Both these angles are substantially higher than the corresponding static angles (see Table 2).

As the airfoil pitches past the dynamic stall angle, the flow becomes largely separated and the separating leading-edge shear layer grows unstable, forming several vortices as can be seen from the bottom row frames in both Figs. 2 and 3. The flow downstream of the trailing edge also shows several small organized vortical structures. Occasionally (Fig. 2, $\alpha = 28$ deg) a trailing vortex (much like the starting vortex) can be seen coming off the trailing edge of the airfoil during the deep stall phase of the flow.

Figure 4 presents an enlarged schlieren photograph for $M = 0.25$, $\alpha^+ = 0.025$, at $\alpha = 16.5$ deg. At this condition some interesting details are present in the flow. As already stated, the forward stagnation point is on the lower surface at about 5% chord point. On the upper surface there is a large dynamic stall vortex at $x/c \approx 0.5$. Along with it is another structure which appears to have the same sense of vorticity as the dynamic stall vortex. Downstream of the primary vortex, the flow is still attached. It is surprising to see two clockwise vortical structures at the same time. Chandrasekhara et al.[18]

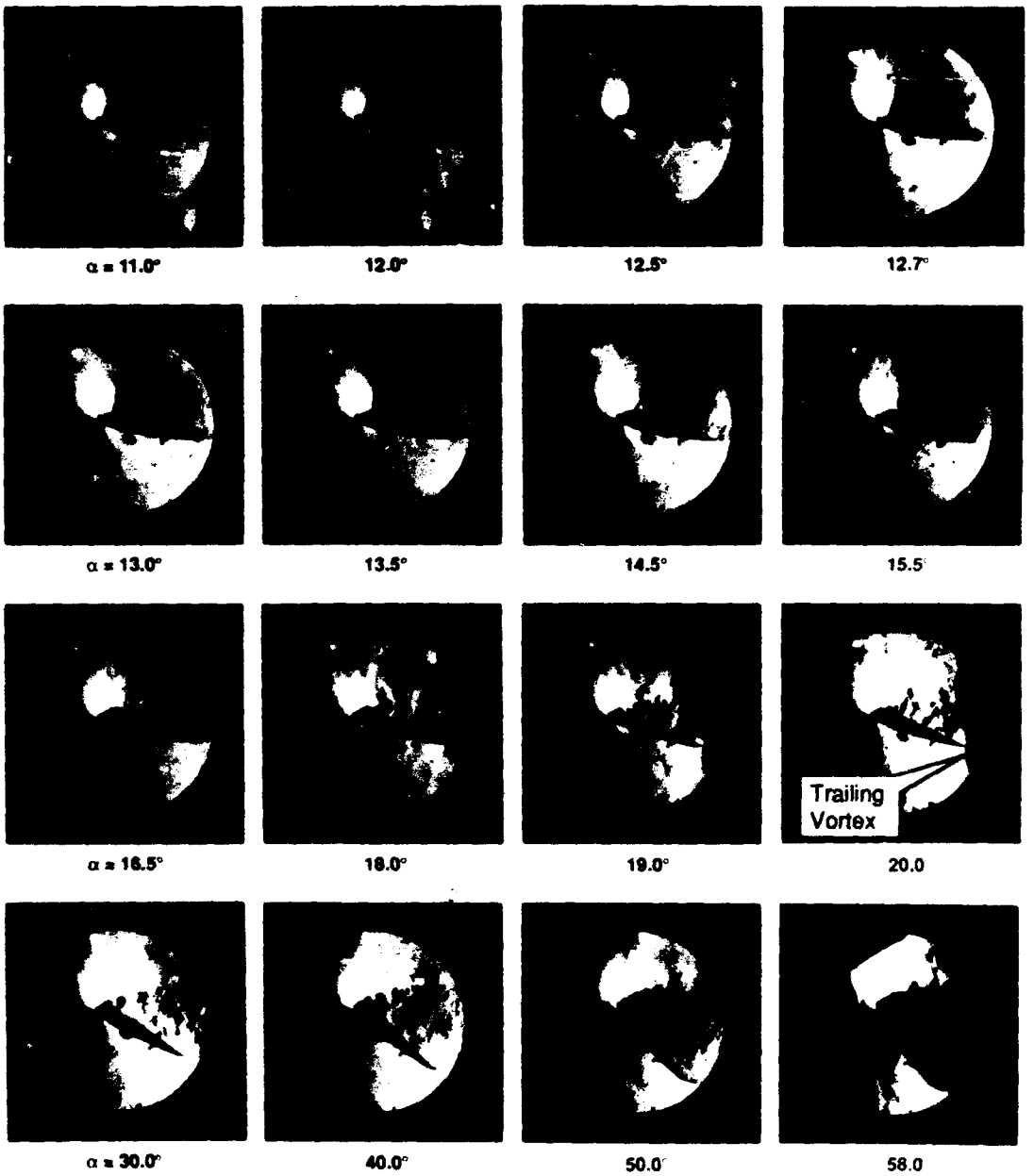

Fig. 3 Stroboscopic schlieren photographs of the compressibility effects on dynamic stall of a rapidly pitching airfoil: $M = 0.45$, $\alpha^+ = 0.03$.

have detected such structures in their computational studies of the flow over an oscillating airfoil under compressibility conditions. Mane et al.[19] have also found such structures in their computational studies on pitching airfoils, but at a low Reynolds number of 50,000. At this stage it is not known whether the multiple structures would influence dynamic lift generation in any way. However, these seem to appear mostly at low Mach numbers and only at low pitch rates.

Another noteworthy feature is the large vertical length scale of the flow. It appears that the vortex diffuses and rapidly becomes disorganized as it moves over the airfoil. In contrast, studies of the flowfield over an oscillating airfoil by Chandrasekhara and Carr[16] have shown that the vortex was very tightly wound. Chandrasekhara et al.[17] have compared the effect of motion history and found that in the range of parameters tested, the ramp-type motion is not very effective in introducing the levels of vorticity that can be attained by the oscillating motion due to the fact that the integrated effect of pitch rate history on vorticity generation is larger in the oscillating case. This is a possible explanation for the observed structure of the dynamic stall vortex in this case.

B. Formation of Shocks over the Airfoil

Figure 5 shows the details of the flow near the leading edge of the airfoil for $M = 0.45$, $\alpha^+ = 0.0313$, $\alpha = 12.6$ deg. The strong density gradients near the airfoil leading edge under these conditions are responsible for deflecting the light rays completely away from the region, which results in a dark region seen on the upper surface in this figure. The most striking result seen in the figure is the presence of multiple shocks within the first 5–8% chord distance. The rapid acceleration of the flow around the leading edge for this case has caused the flow to go supersonic. Such a result has also been indicated in computational studies. The extent of the supersonic region depends upon the Mach number, nondimensional pitch rate, and instantaneous angle of attack. For example, Visbal[11] found that a supersonic region originates very near the leading edge and extends until about 8–10% chord point for $M = 0.3$, and it grows to about 30% chord at $M = 0.6$. The results obtained from the present study offer the first definitive experimental documentation of the fact that shocks actually form on the airfoil for certain flow conditions and support the study by Visbal,[11] with the exception of the formation of multiple shocks. It is well known that once a flow attains supersonic values, a shock can form. In the present case, it is not known whether the shock is normal or oblique, but presence of multiple shocks indicates that if a normal shock originally formed, there are additional mechanisms present in the flow that are responsible for accelerating the flow repeatedly to supersonic values and this subsequently forms more shocks. A possible explanation is that the shock induces small scale separation in the boundary layer. The

Table 2 Vortex release angle of attack

	α^+							
M	0[a]	0.01	0.02	0.025	0.03	0.035	0.04	0.05
0.20				17.5		21.0	22.0	24.0
0.25				17.5	18.5	21.0	22.0	27.0
0.30	12.4		17.5	18.0	20.0	21.0	23.0	
0.35	11.6		16.0	17.5	19.0	20.0	23.0	
0.40	10.8		15.5	17.0	19.0	20.0		
0.45	9.5	12.0	15.5	17.0	18.0			

[a]Best estimate of static stall angle from schlieren photographs.

Fig. 4 Multiple vortices on a pitching airfoil: $M = 0.25$, $\alpha^+ = 0.025$, $\alpha = 16.5$ deg.

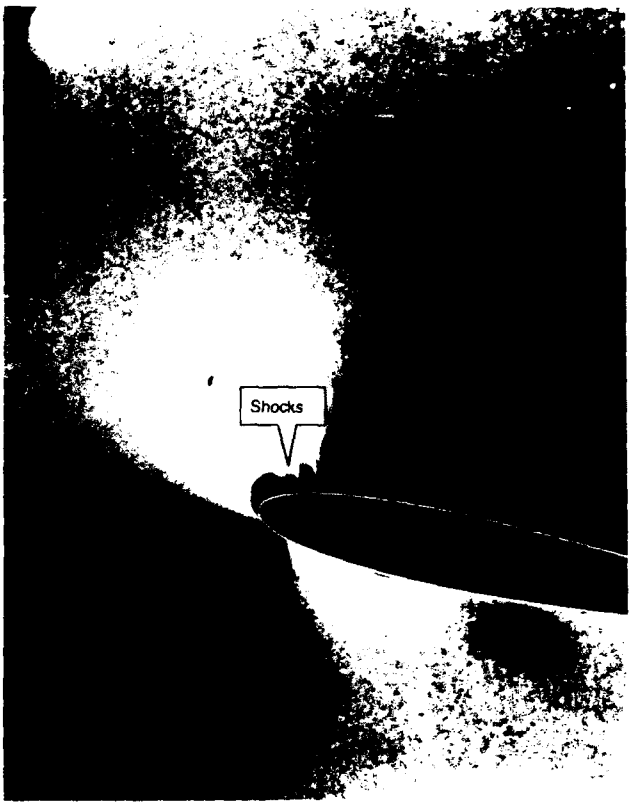

Fig. 5 Schlieren photographs of multiple shocks on a rapidly pitching airfoil: $M = 0.45$, $\alpha^+ = 0.0313$, $\alpha = 12.6$ deg.

separating streamlines could take a wavy shape and locally induce a series of expansion and compression waves. Such a system of waves could form additional shock waves (or shocklets) in the flow. Eventually the series of interactions ceases by way of a "strong" shock and the flow becomes subsonic. This explanation still needs to be verified, but such a situation seems possible in transonic flow.

The shocks discussed above were also present over a range of angles of attack at $M = 0.45$ from 12.2–12.9 deg. However, no large scale shock-induced separation could be detected for any of the cases studied. In fact, the dynamic stall vortex still formed and was eventually shed at $\alpha = 17$ deg.

C. Effect of Mach Number

Figure 6 compares the schlieren photographs at different Mach numbers for $\alpha^+ = 0.03$ and $\alpha = 17$ deg. It can be seen that for the subsonic case ($M \leq 0.3$), the vortex is at about 50% chord location. In addition, the vertical extent of the flow is nearly the same for $M = 0.2$, 0.25, and 0.3. However, for $M \geq 0.3$, the dynamic stall vortex moves successively closer to the trailing edge and the flow scales have increased as well. Movement of the vortex downstream indicates flow approaching the deep stall state and, therefore, it is clear from the figure that as the Mach number is increased deep stall occurs at progressively lower angles of attack.

Figure 7a shows the effect of Mach number on dynamic stall for $\alpha^+ = 0.025$, and the corresponding results for $\alpha^+ = 0.035$ are shown in Fig. 7b. Plotted in it are the successive locations of the center of the dynamic stall vortex as a function of the instantaneous angle of attack at different Mach numbers. It can be seen in both of these figures that the vortex appears at lower angles of attack as the Mach number increases. This also leads to the result that the vortex moves past the trailing edge at lower angles of attack for higher Mach numbers causing deep dynamic stall to occur earlier in the pitching cycle. Significant decreases in the angle of attack occur for the same x/c location for $M \geq 0.3$ and thus, $M = 0.3$ can be considered to be the limit when compressibility effects set in. Consider, e.g., Fig. 7a, the center of the vortex is at $x/c \approx 0.6$ when $\alpha = 16.5$ deg for $M = 0.3$, and at $\alpha = 14$ deg for $M = 0.45$. Similarly, in Fig. 7b the vortex is at 60% chord location at $\alpha = 19$ deg for $M = 0.3$; at $M = 0.4$, the corresponding angle of attack = 17.2 deg. Similar results were obtained at other pitch rates.

Table 2 shows the angle of attack at which deep dynamic stall occurs for the cases studied. As the Mach number is increased for a given pitch rate, the dynamic stall angle remains nearly the same up to $M = 0.3$. However, for $M \geq 0.3$, this angle decreases. The scatter that is present in the data is unavoidable, owing to the subjectiveness involved in determining these angles. Furthermore, as stated in Sec III.A, for some cases multiple structures were found to be present. This, along with the diffused vortex, made the task of tracking the vortex movement more complex. Nevertheless, the data shows definitive trends that reflect the compressibility effects.

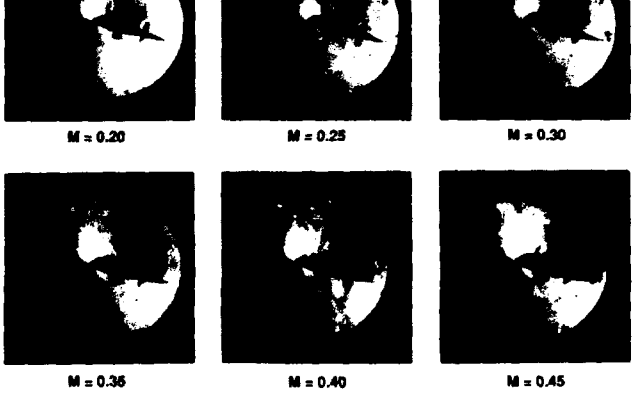

Fig. 6 Effect of Mach number on dynamic stall of a rapidly pitching airfoil, schlieren studies: $\alpha^+ = 0.03$, $\alpha = 17$ deg.

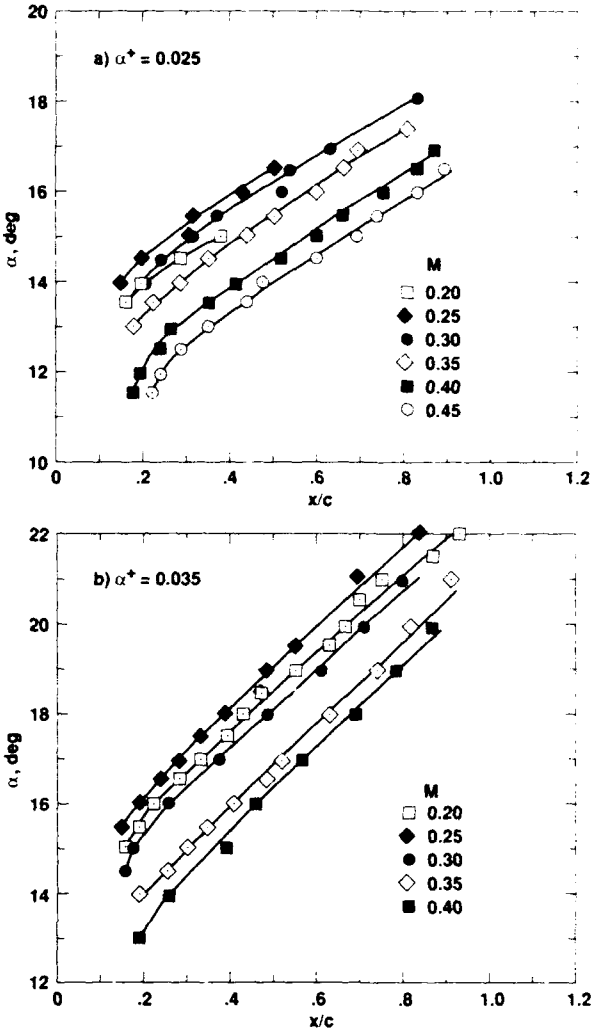

Fig. 7 Quantitative effects of Mach number on dynamic stall vortex location.

D. Effect of Pitch Rate

Figures 8a–d show the vortex center locations over the airfoil plotted as a function of the angle of attack at different pitch rates for $M = 0.2$, 0.35, 0.4, and 0.45, respectively. It can be seen in all the figures that the vortex is retained on the surface of the airfoil to higher angles of attack as the pitch rate is increased. The trend is monotonic with increasing pitch rate. For example at $M = 0.45$ the vortex is on the surface even at $\alpha = 18$ deg at $\alpha^+ = 0.03$, whereas, the static stall angle for this case is ≈9.5 deg as determined from the schlieren images. For $\alpha^+ = 0.020$, deep dynamic stall occurs at $\alpha = 15.5$ deg. For $M = 0.35$, the deep stall angle is ≈23 deg for $\alpha^+ = 0.04$, and the static stall angle is 11.6 deg. The figures show similar results for other Mach numbers. A summary of dynamic stall angles is presented in Table 2 at different pitch rates. A horizontal scan of the table shows that stall delay until angles of attack significantly higher than the static stall angles can be achieved by simply increasing the nondimensional pitch rate, even at these higher Mach numbers. As indicated in the previous section, the presence of multiple structures, especially at the low Mach number of 0.2, made following the primary vortex during its passage over the airfoil difficult. Hence, the plot for $\alpha^+ = 0.025$ in Fig. 8a does not show the deep stall angle of attack.

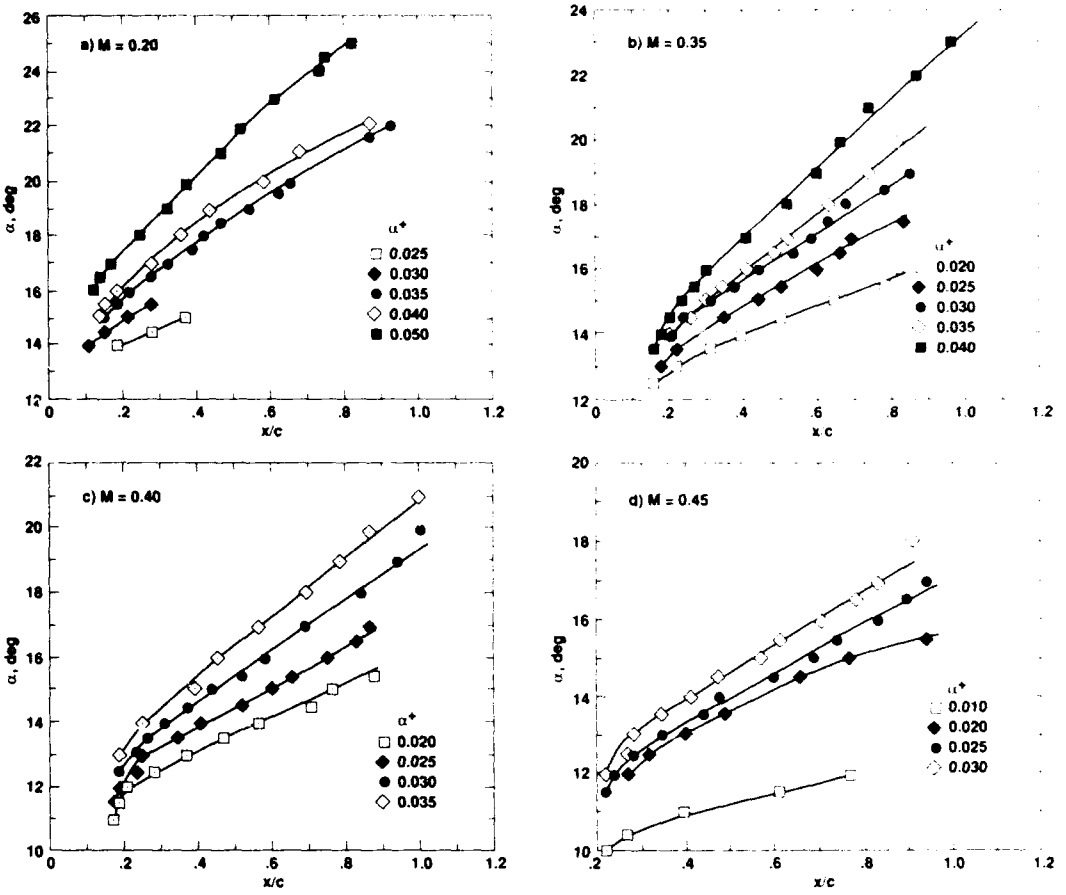

Fig. 8 Quantitative effects of pitch rate on dynamic stall vortex location.

IV. Concluding Remarks

Results obtained showing the global behavior of the dynamic stall vortex over an airfoil executing a rapid transient pitching motion are presented. These are the first pictures of the dynamic stall flowfield obtained at maneuver Mach number conditions and for conditions that are beyond the operational range of present day aircraft.

The following major conclusions could be drawn from the study:

1) Multiple shocks are present over the airfoil, at $M = 0.45$, at $\alpha^+ = 0.0313$, and at an angle of attack = 12.6 deg. The shocks do not seem to induce any large scale flow separation. Also, the global features of the dynamic stall process are not significantly affected by their presence. However, detailed studies are still needed to confirm local effects of the shocks.

2) At a low Mach number of 0.25, and a low nondimensional pitch rate of 0.025, multiple vortices are present over the airfoil surface. But at higher Mach numbers, a single large dynamic stall vortex dominates the flow. Occasionally a trailing vortex similar to the starting vortex is observed.

3) Compressibility effects are important for $M \geq 0.3$.

4) Stall delay is enhanced by increasing the pitch rate, even when compressibility effects are present. Increasing Mach number accelerates dynamic stall by decreasing the angle of attack at which dynamic stall occurs.

Acknowledgments

The project was supported by AFOSR-MIPR-87-0029 and 88-0010 (monitored by H. Helin) with additional support from NAVAIR (T. Momiyama) and ARO (T. L. Doligalski). The technical support of Michael J. Fidrich and the staff of the NASA Fluid Mechanics Laboratory is greatly appreciated.

References

[1]Carr, L. W., "Progress in Analysis and Prediction of Dynamic Stall," *Journal of Aircraft*, Vol. 25, No. 1, 1988, pp. 6–17.

[2]McCroskey, W. J., "The Phenomenon of Dynamic Stall," NASA TM 81264, March 1981.

[3]Freymuth, P., "Vortex Patterns of Dynamic Separation," *Encyclopedia of Fluid Mechanics*, edited by N. P. Cheremisinoff, Gulf Publishing, Houston, TX, Vol. 8, 1989, Chap. 11.

[4]Lorber, P. F., and Carta, F. O., "Unsteady Stall Penetration Experiments at High Reynolds Number," Air Force Office of Scientific Research TR-87-1202, East Hartford, CT, April 1987.

[5]Albertson, J. A., Troutt, T. R., and Kedzie, C. R., "Unsteady Aerodynamic Forces at Low Airfoil Pitching Rates," *Proceedings of the 1st National Fluid Dynamics Congress*, AIAA Paper 88-2579-CP, Cincinnati, OH.

[6]Walker, J. M., Helin, H. E., and Strickland, J. H., "An Experimental Investigation of an Airfoil Undergoing Large Amplitude Pitching Motions," *Journal of Aircraft*, Vol. 23, No. 8, 1985, pp. 1141, 1142.

[7]Francis, M. S., and Keese, J. F., "Airfoil Dynamic Stall Performance with Large-Amplitude Motions," *Journal of Aircraft*, Vol. 23, No. 11, 1985, pp. 1653–1659.

[8]Jumper, E. J., Dimmick, R. L., and Allaire, A. J. S., "The Effect of Pitch Location on Dynamic Stall," *Journal of Fluids Engineering, Trans. ASME*, Vol. 11, No. 3, 1989, pp. 256–262.

[9]Harper, P. W., and Flanigan, R. E., "The Effect of Rate of Change of Angle of Attack on the Maximum Lift of a Small Model," NACA TN 2061, Hampton, VA, March 1950.

[10]Ekaterinaris, J. A., "Compressible Studies of Dynamic Stall," AIAA Paper 89-0024, Reno, NV, Jan. 1989.

[11]Visbal, M. R., "Effect of Compressibility on Dynamic Stall of a Pitching Airfoil," AIAA Paper 88-0132, Reno, NV, Jan. 1988.

[12]McCroskey, W. J., McAlister, K. W., Carr, L. W., Pucci, S. L., Lambert, O., and Indergrand, R. F., "Dynamic Stall on Advanced Airfoil Sections," *Journal of American Helicopter Society*, Vol. 26, No. 3, pp. 40–50.

[13]Carr, L. W., and Chandrasekhara, M. S., "Design and Development of a Compressible Dynamic Stall Facility," *Journal of Air-*

craft, Vol. 29, No. 3, 1992, pp. 314–318.

[14]Andrews, D. R., "An Airfoil Pitching Apparatus: Modeling and Control Design," 35th Instrument Society of America International Instrumentation Symposium, Orlando, FL, May 1989.

[15]Chandrasekhara, M. S., and Carr, L. W., "Design and Development of a Facility for Compressible Dynamic Stall Studies of a Rapidly Pitching Airfoil," *Proceedings of the 13th ICIASF Conference*, Goettingen, Germany, Sept. 18–21, 1989.

[16]Chandrasekhara, M. S., and Carr, L. W., "Flow Visualization Studies of the Mach Number Effects on the Dynamic Stall of an Oscillating Airfoil," *Journal of Aircraft*, Vol. 27, No. 6, 1990, pp. 516–522.

Chandrasekhara, M. S., Carr, L. W., and Ahmed, S., "Comparison of Pitch Rate History Effects on Dynamic Stall," *Proceedings of NASA/AFOSR/ARO Workshop on Physics of Forced Unsteady Separation*, NASA CP 3144, Moffett Field, CA, April 1990.

Chandrasekhara, M. S., Ekaterinaris, J. A., and Carr, L. W., "Experimental and Computational Tracking of Dynamic Stall Vortex," *Bulletin of the American Physical Society*, Vol. 33, No. 10, 1988, p. 2251.

Mane, I., Loc, T. P., and Werle, H., "Sur le Decollement Instationnaire Autour d'un Profil a Grands Nombres de Reynolds: Une Comparison Calcul Experience," *Mecanique des Fluides*, Academie des Sciences, 305, Series II, Paris, France, 1987, pp. 229–232.